

## Research paper

## Performance analysis of thermoelectric generator implemented on non-uniform heat distribution of photovoltaic module

Ruzaimi A. <sup>a,\*</sup>, Shafie. S <sup>a,b</sup>, W.Z.W. Hassan <sup>a,b</sup>, N. Azis <sup>a,b</sup>, M. Effendy Ya'acob <sup>c</sup>, E. Elianddy <sup>d</sup>, Aimrun W. <sup>e</sup><sup>a</sup> Institute of Advanced Technology (ITMA), Universiti Putra Malaysia (UPM), Malaysia<sup>b</sup> Department of Electrical & Electronic Engineering, Faculty of Engineering, Universiti Putra Malaysia (UPM), Malaysia<sup>c</sup> Department of Food & Processing Engineering, Faculty of Engineering, Universiti Putra Malaysia (UPM), Malaysia<sup>d</sup> Department of Mechanical & Manufacturing Engineering, Faculty of Engineering, Universiti Putra Malaysia (UPM), Malaysia<sup>e</sup> Department of Biological and Agricultural Engineering, Faculty of Engineering, Universiti Putra Malaysia (UPM), Malaysia

## ARTICLE INFO

## Article history:

Received 13 December 2020

Received in revised form 25 March 2021

Accepted 16 April 2021

Available online xxxx

## Keywords:

Photovoltaic (PV)

Solar system

Thermoelectric (TE)

Thermoelectric generator (TEG)

Greenhouse system

Agrivoltaic

## ABSTRACT

PV–TEG hybrid system is widely discussed nowadays, as an alternative way to maximize solar radiation energy which is from both of its light and heat. In recent years, the idea of using thermoelectric generators (TEGs) to extract energy from heat waste has increased with applications varying from milliwatts to kilowatts. To form a circuit, numbers of TEG modules can be connected in series and/or parallel configuration to produce the required voltage and/or current. In the PV–TEG systems, due to operating environments, each TEG module's power generation is subject to temperature mismatch. There is also considerable variability in the electro-thermal output and mounting pressure of each TEG module in a circuit, resulting in a significant inconsistency. Therefore, when each TEG in the array is active, a varying electrical operating point will occur at which peak energy can be obtained and problems with lower power output will occur. In this work, an individual TEG module test method was used to measure and analyze data from specific types of TEG, and a record of the maximum power output under different temperature variations is obtained. Then, the performance of the TEG system is measured and evaluated with a test bench where the modules are attached at different backside areas of generic PV panels. The non-uniform heat distribution condition created in the experiment showed an average 33 % drop in power production from the maximum power that would be available in case each TE series circuit operates under uniform heat distribution. This experimental finding demonstrates the problem and the outcomes discussed in this paper validated a thorough examination of the effect of nonuniform operating temperatures on a range of thermoelectric generator's energy output.

© 2021 The Authors. Published by Elsevier Ltd. This is an open access article under the CC BY-NC-ND license (<http://creativecommons.org/licenses/by-nc-nd/4.0/>).

## 1. Introduction

Developing clean, reproducible, and environmentally friendly energy is essential in today's increasing demand for energy and due to natural resource depletion. Solar energy is the biggest future clean energy resource in the form of light and heat that can be directly converted to electricity. The combination of photovoltaic (PV) and thermoelectric generator (TEG) technology has been critically discussed throughout the previous decade and has proved to be a useful solution to use solar waste heat in enhancing energy output effectiveness compared to single PV systems. Through the Seebeck effect, TEG modules can directly convert excess thermal energy into electrical energy through the temperature difference between the PV back contact (which serves as

the TEG heat input) and the TEG cold junction. Moreover, the use of TEG has many benefits as its heat composition is static, totally silent, clean and, comparable to PV systems, can last for years.

Today, many thermoelectric materials are being explored to improve and optimize power generation. Naor Madar et al. (2016) in their research focusing on the potential doping of *p*-type GeTe-rich alloy to the Bi<sub>2</sub>Te<sub>3</sub> at ~9% solubility limit, achieved an electronic optimization at maximal thermoelectric figure of merit, ZT, ~1.55 at ~410 °C (Madar et al., 2016). Their method was precedent from research by Yaniv Gelbstein et al. (2014), where they used density functional theory and analytical modeling, approaches the lattice thermal conductivity values originated solely by alloying/disordering effects in the highly thermoelectrically efficient *p*-type Ge<sub>x</sub>Pb<sub>1-x</sub>Te alloys (Gelbstein et al., 2014). ZT enhancement of up to 40% reported by Ben-Ayoun et al. (2017), in which where they were using hot-pressing synthesis rather

\* Corresponding author.

E-mail addresses: [mohdruzaimi@gmail.com](mailto:mohdruzaimi@gmail.com) (Ruzaimi A.), [suhaidi@upm.edu.my](mailto:suhaidi@upm.edu.my) (Shafie. S).

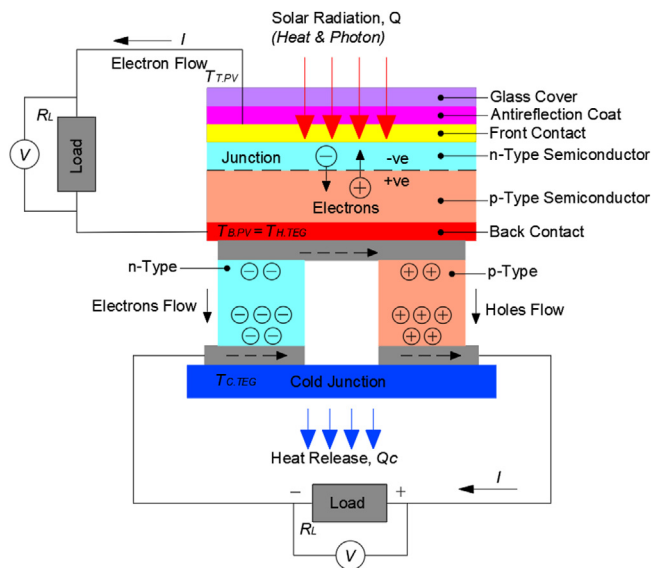


Fig. 1. Electrical equivalent circuit of PV-TEG hybrid system.

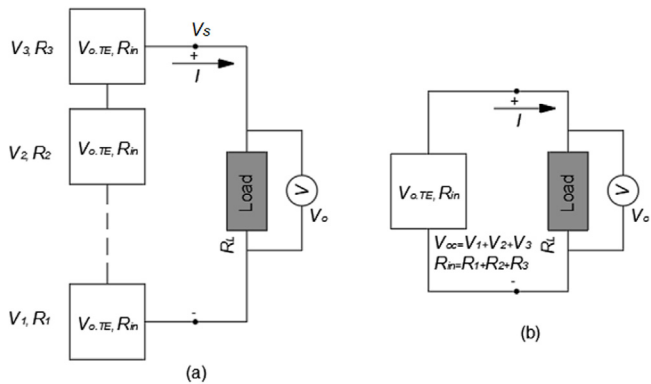


Fig. 2. Electrical equivalent circuit of three TEG modules connected in series (a); and its equivalent summation (b).

than the previously reported cold pressing and sintering for *n*-type doped PbTe and *p*-type alloys. They found that in this class of TE materials, sublimation of volatile species from grain boundaries was apparent, degrading the TE figure of merit (Ben-Ayoun et al., 2017). While in another works by Meroz et al. (2016), in their study, Bi<sub>2</sub>Te<sub>2.4</sub>Se<sub>0.6</sub> composition was optimized by CH<sub>3</sub> doping, preferred alignment of the crystallographic orientation, and lattice thermal conductivity minimization achieved a maximal ZT of ~0.9, obtained at ~175 °C highest reported for *n*-type Bi<sub>2</sub>Te<sub>x</sub>Se<sub>3-x</sub> based alloys (Meroz et al., 2016). Sadia et al. (2014) in their research achieved maximum ZTs of ~0.5 for the doped stoichiometric *p*-type higher manganese silicides (HMS) (FeSi<sub>2</sub>)<sub>0.05</sub>(MnSi<sub>1.73</sub>)<sub>0.95</sub> composition without any Silicide (Si) excess (Sadia et al., 2014).

In a TEG system, several thermoelectric modules are connected to the required power level in a series and parallel array. The electrical energy generated by TEG varies for a given heat operating point depending on the current obtained by the electrical load. The temperature of each thermoelectric module is non-even in most TEG systems. Examples of cases where this non-even heat distribution happened as discovered in exhaust systems or where the mechanical system's thermal conductivity is poorly regulated (Montecucco et al., 2012). The TEG's mechanical mounting pressure contributes indirectly to variability in the electrical

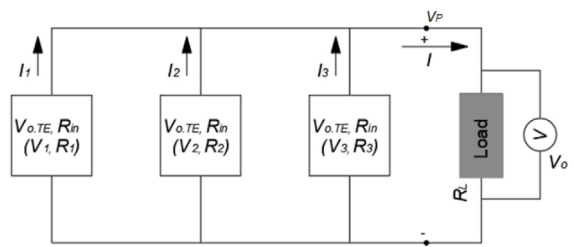


Fig. 3. Electrical equivalent circuit of three TEG modules connected in parallel.

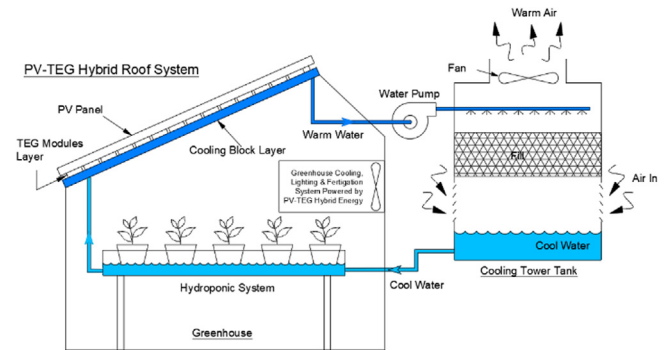


Fig. 4. Proposed PV/TEG Greenhouse System Concept utilizing Hydroponic System for TEG cooling.

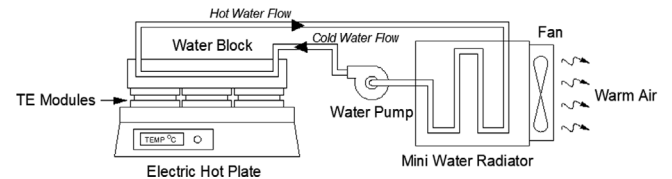


Fig. 5. Thermoelectric module performance experiment set-up.

output due to dissimilarity with the partly pressure-dependent thermal contact resistance. Therefore, each TEG module in the array will have a different *P*<sub>max</sub> when in operation. For optimum output, each TEG should be operated and controlled separately, but this will significantly increase the quantity and complexity of the required electronic converters and adversely impact the system application cost.

In this work, an individual TEG module test method was used to measure and analyze data obtained from three common types of TEG, all of which were reported to be highly efficient in low-temperature applications. The effect of applying a clamping force to the modules is addressed, and a record of the maximum power output under different temperature variations is obtained. Then, based on the results of individual module experiments, the performance of the TEG system (TEGs connected electrically in series and parallel) is measured and evaluated with a test bench where the modules are attached to the backside of generic PV panels. The power loss as a result of mismatched conditions is quantified and discussed. The suggested approach for improving the TEG system's efficiency is discussed in the following sections.

## 2. PV-TEG hybrid system & development

Fig. 1 represents the electrical circuit of a PV-TEG hybrid system which combined PV and TEG module with isolated power output. Solar radiation or sunlight, *Q* illuminate the PV cell generating electrical power, *P*<sub>PV</sub>. The radiation that is not converted into electrical energy, conducts heat, *T*<sub>PV</sub> transferring it to TEG's

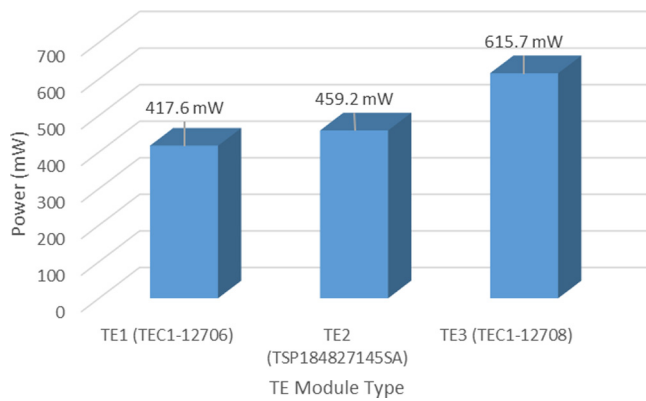


Fig. 6. TE power output at  $\Delta T$  40 °C (hot side 80 °C, cold side 40 °C)

hot side  $T_{H,TEG}$ , converting it to additional electrical power,  $P_{TEG}$ , and removed from the system via the TEG's cold side,  $T_{C,TEG}$ . The total electrical power output of the system,  $P_{PV,TEG}$ , and efficiency,  $\eta_{PV,TEG}$  is given by Eqs. (1) and (2):

$$P_{PV,TEG} = P_{PV} + P_{TEG} \quad (1)$$

$$\eta_{PV,TEG} = \frac{P_{PV,TEG}}{Q} \quad (2)$$

where  $P_{PV}$  and  $P_{TEG}$  are the power output of the PV and TEG module respectively, while  $Q$  is the solar irradiance incident input energy equal to  $Q=I_s A$  where  $I_s$  is the solar intensity illuminating the top surface of a solar module with an area,  $A$ .

The earliest development of this hybridization has been proven by van Sark (2011) by applying a roof-mounted PV–TEG hybrid system model to evaluate the system efficiency by mounting the TEG modules directly to the backside of PV modules, focusing on the combined electrical output. 11–14.7% increase in efficiency claimed in this system (van Sark, 2011). A combination of a series-connected dye-sensitized solar cell (DSSC), a solar selective absorber (SSA) and a TEG module was established by Wang et al. (2011) which results between 9.39%–13.8% efficiency increment (Wang et al., 2011). Whereas, efficiency from 16.5%–22.02% has been reported by Hsueh et al. (2015) in their series-connected CuInGaSe2 (CIGS) PV cell with a TEG module (Hsueh et al., 2015). Lin et al. (2015) experimented with the load matching in a PV–TEG hybrid system and the results proved that the solar irradiance, load resistances, and structure parameters of the TEG were correlated with the optimum performance of the

hybrid system (Lin et al., 2015). In another study, Zhu et al. (2016) constructed a PV–TEG hybrid system with thermal concentrated and optimized thermal management. They embraced copper plates that serve as a heat concentrator and conductor that generate a big temperature difference between the two sides of TEG modules. This system has accomplished indoor experiment effectiveness of 23% greater compared to a single PV cell system (Zhu et al., 2016).

Most of the prior research related to the PV–TE hybrid system was assumed based on continuous incident solar radiation where the solar radiation and temperature in the real climate differ at all times. This article introduces the feasible application of the TEG-Hybrid system in a fluctuating temperature setting and how the distribution of heat can affect the TEG circuit energy output. Tang et al. (2015) researched the electrical performance of TEG systems under mismatch conditions, such as restricted working temperature and inconsistent temperature distributions across modules connected in series. They concluded that applying sufficient mechanical pressure to the module enhances electrical efficiency. The power loss of the modules in series connection is significant, 11% less than the theoretical calculated power, as a result of the non-uniform temperature condition (Tang et al., 2015). It also has been proven by a theoretical analysis presented by Montecucco et al. (2014) that the electro-thermal effects that occur in series and parallel arrays of thermoelectric generators when the individual module are exposed to non-uniform temperature gradients may have a significant impact on the performance of the thermoelectric system (Montecucco et al., 2014).

### 3. TEG array configuration

Normally, the TEG circuit or system was set up in series and/or parallel interconnection arrays in a thermoelectric system to produce higher voltage and current levels. The arrangement of the TEG circuit combination is usually determined by the voltage and/or current requirements.

#### 3.1. Series connection

TEG modules can be considered as a dependent power source as each module provides a voltage supply whose magnitude depends on either the voltage across or current flowing through some other circuit element. When it comes to the series circuit, different voltage inputs can be used as long as there are other circuit elements in between to comply Kirchhoff's Voltage Law (KVL). Fig. 2 shows three TEG connected in series, each representing voltage source  $V_1$ ,  $V_2$  and  $V_3$ , with an internal resistance

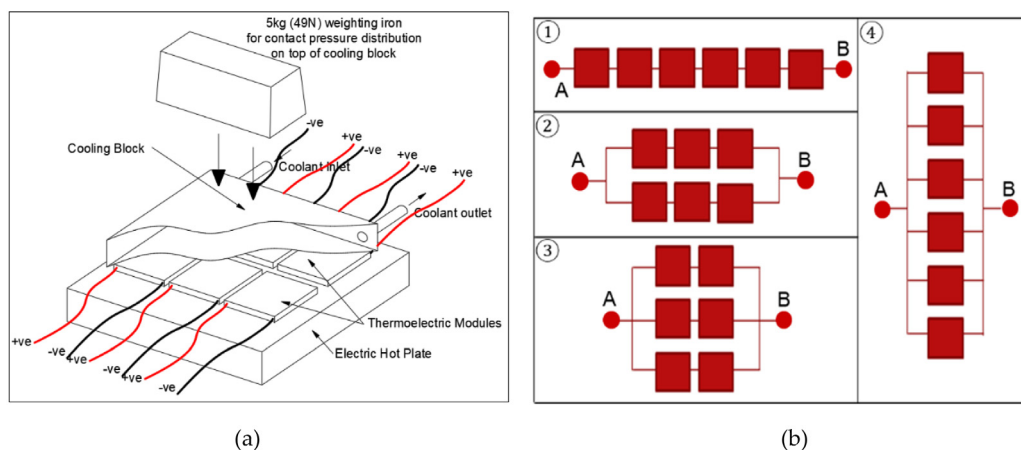


Fig. 7. (a) Illustration of the experimental set-up for thermoelectric series-parallel array performance; (b) Array configuration setup for TEG series-parallel measurement.

( $R_{in}$ ) of  $R_1$ ,  $R_2$  and  $R_3$ . In a series aiding voltage source where the current flow in the same direction, each module in the array will encounter an equal  $\Delta T$  under ideal operating conditions. Therefore all modules will generate an equivalent output voltage,  $V_1=V_2=V_3$ , and the array will be in a balanced thermal state. Total source voltage,  $V_s = V_1+V_2+V_3$ , and in this case, total  $R_{in} = R_1 + R_2 + R_3$  while current,  $I = V_s/(R_{in})$ . Thus, the maximum power,  $P_{max}$  can be written as:

$$P_{max} = I^2(R_{in}) \quad (3)$$

However, in a practical system, real thermal operating conditions may be such that each TEG may encounter a different range of  $\Delta T$  and therefore their voltages and internal resistance will not be equal.

### 3.2. Parallel connection

Fig. 3 represents the parallel setup of three TEG. The TEG modules in the circuit operate on the same  $\Delta T$  under optimal operating conditions. Therefore, each TEG generates the same voltage and current, operating at maximum power with  $I_1 = I_2 = I_3$ . The varying  $\Delta T$  across each TEG module can result in a difference in the current magnitude under non-ideal thermal conditions:

$$I_1 = \frac{V_1 - V_p}{R_1} \quad (4)$$

$$I_2 = \frac{V_2 - V_p}{R_2} \quad (5)$$

$$I_3 = -I_1 - I_2 \quad (6)$$

where  $V_p$  is the voltage at the array's terminal.

## 4. Experimental analysis of thermoelectric generator performance

Previous research by Ruzaimi et al. (2018) where PV/TEG Hybrid Greenhouse System conceptual design was considered (Ariffin et al., 2017). This system utilizes the waste heat from the greenhouse PV roof panels by integrating the TEG system on its backside and using the circulating fertilizer water as the liquid coolant for the TEG's cold side source ( $T_{C,TEG}$ ) to get the  $\Delta T$  to generate electrical power. Fig. 4 shows the reformed concept of the PV/TEG Greenhouse System proposed.

### 4.1. Experiment 1: Individual preliminary test for thermoelectric module type selection

This experiment purpose is to compare the performance of three different types of common TE modules which have high ZT, proven in plenty research works to be reliable and effective in a low-temperature application (Çimen et al., 2017; S. and Tahir, 2018). Table 1 gives some characteristics of those three different modules.

Fig. 5 shows the experimental setup for the thermoelectric module test. The thermoelectric modules are clamped between the liquid cooling block and the electric hot plate. A hot plate provides an emulated heat that is proportional to the voltage applied. Aluminum liquid cooling blocks were used as a heat exchanger with coolant (water) flowing through to regulate the thermoelectric module's cold temperature. The coolant is pumped at a set temperature from a constant-temperature mini-chiller tank. The temperature of the coolant is controlled by the mini chiller's PID controller.

Based on the recent concept proposed in a study conducted by Ruzaimi et al. (2018) in their literature (Ruzaimi et al., 2018), an

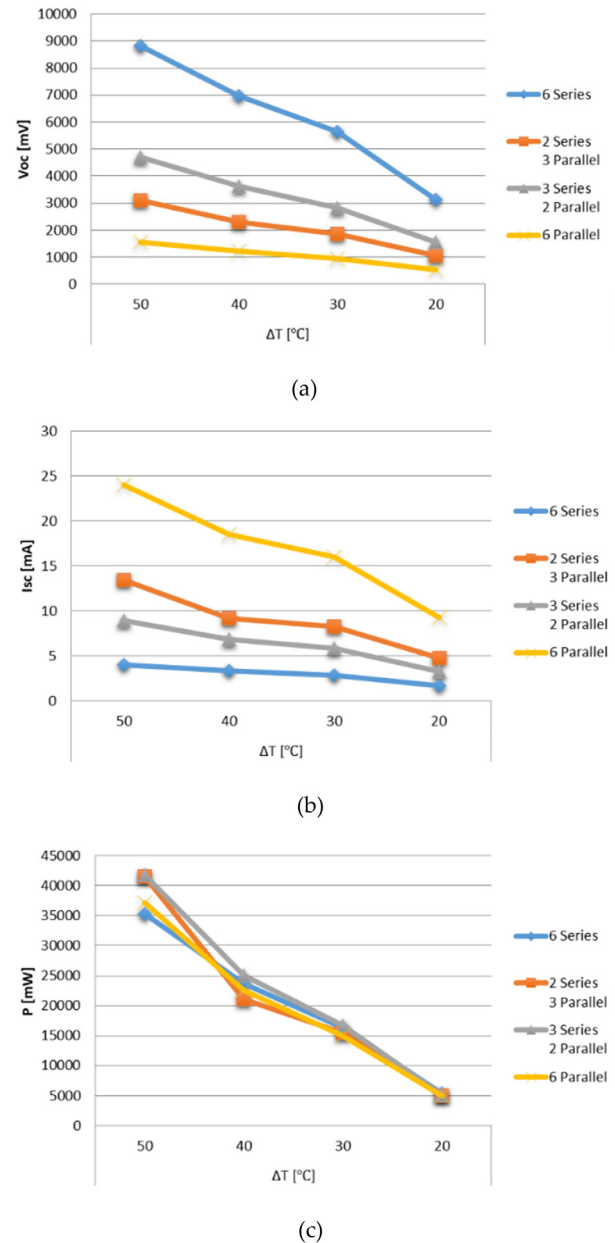


Fig. 8. (a) Open circuit voltage (Voc) vs. temperature difference ( $\Delta T$ ); (b) Short circuit current (Isc) vs. temperature difference ( $\Delta T$ ); (c) Output power (P) vs. temperature difference ( $\Delta T$ ). (For interpretation of the references to color in this figure legend, the reader is referred to the web version of this article.)

observation was done by setting the temperature of the hot side of TE modules to the maximum PV panel's backside temperature recorded, which is  $80^{\circ}\text{C}$  and the temperature at the cold side at  $40^{\circ}\text{C}$ . This experimental set-up was built to compare the maximum power generation of each type at zero loads. The data were compared and the TE module that produces the highest power generated at  $\Delta T$  of  $40^{\circ}\text{C}$  was selected for this PV-TEG hybrid application.

Fig. 6 shows power output for the three types of the thermoelectric module at  $\Delta T 40^{\circ}\text{C}$ , whereby the hot side of the module set to  $80^{\circ}\text{C}$  (which is the maximum average PV temperature) while the cold side was set to  $40^{\circ}\text{C}$  (average ambient temperature underneath the PV panel without any cooling element). It

**Table 1**  
Characteristics of common available thermoelectric.

Details	TEC1-12706		TEC1-12708		SP1848	
Size	40 × 40 × 3.46		40 × 40 × 3.46		40 × 40 × 3.46	
Th (°C)	27	50	25	50	27	50
ΔT max(°C)	70	79	66	75	62	70.6
Vmax (Voltage)	16	17.2	15.4	17.5	3.48	3.88
I <sub>max</sub> (amps)	6.1	6.1	8.5	8.4	9.36	9.24
Q <sub>c</sub> max (Watts)	61.4	66.7	71	79	21.3	23.6
AC resistance (ohms)	2	2.2	1.5	1.8	0.323	–

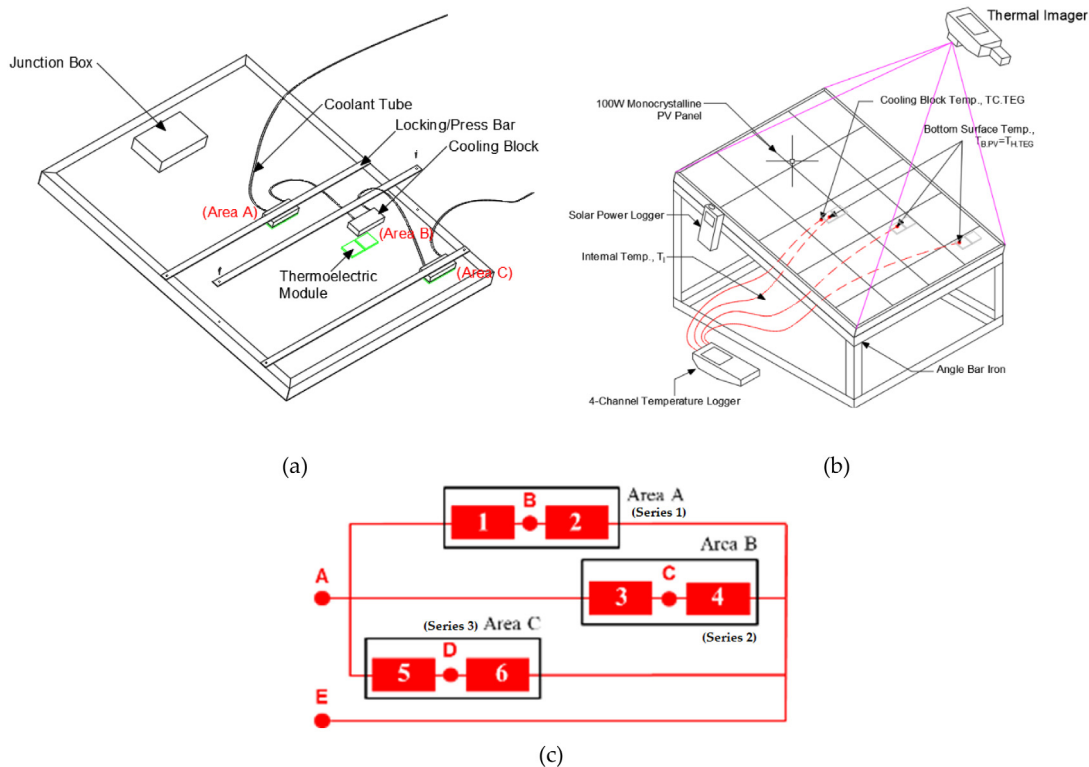


**Fig. 9.** (a) PV Panel Backside Surface with TEG and liquid cooler setup; (b) Data measurement method; (c) TEG series-parallel array at different area.

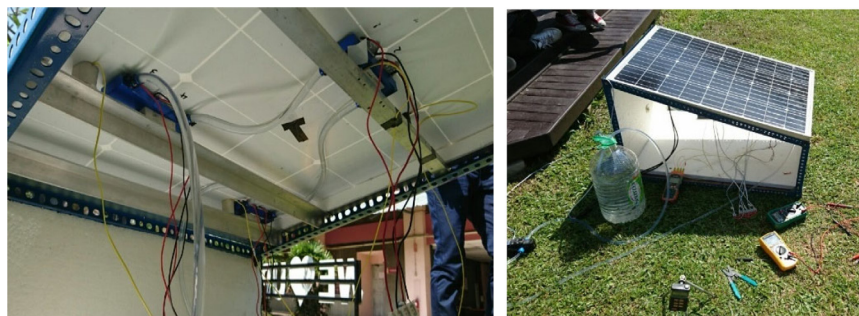


**Fig. 10.** The actual setup at the site shows setup on the PV backside surface (left), and overall view of the setup (right).

can be seen that the highest power output was generated by TE cooler module model TEC1-12708 (TE3) at 615.7 mW, while TE2 produced 459.2 mW and TE1 which is the lowest, producing 417.6 mW.

It is necessary to select the highest power output type of TE modules at low temperatures in this low  $\Delta T$  application. Hence, TE modules from Custom Thermoelectric module TEC1-12708 have been considered for this PV-TEG hybrid application purpose.

#### 4.2. Experiment 2: Series and parallel array configuration

The measurement method described by Montecucco et al. (2013) has been modified to characterize the output of the thermoelectric module in various connection configurations under uniform temperature distribution. Fig. 7(a) shows the setup for the series and parallel array analysis for six numbers of TE modules selected from experiment 1 (TEC1-12706) to measure the

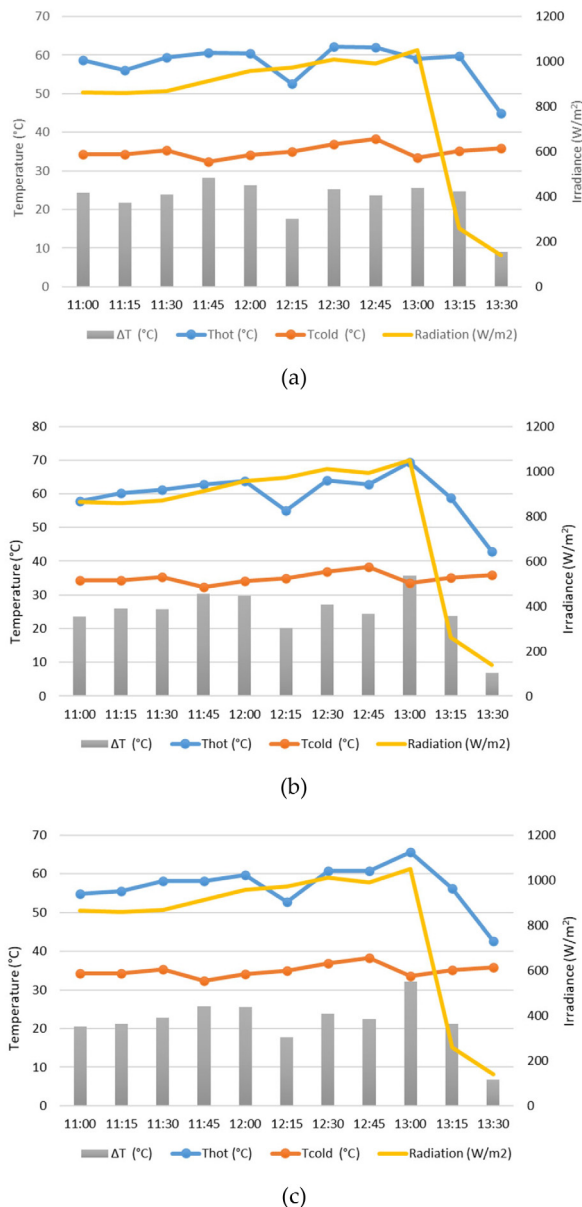


**Fig. 11.** Temperature and solar irradiance level vs. time at (a) Area A; (b) Area B; (c) Area C.

performance output of four configurations under uniform temperature distribution. This test method offers precise and repeatable measurements and allows the mechanical load and temperature uniformity to be controlled independently across each TE module at the same time. The TE modules are sandwiched between the hot plate and a cooling block as in experiment 1. Six TE modules are arranged in 3 x 2 rows and the power is measured by changing the array configuration (Fig. 7(b) which is in; a. 6 series; b. 3 series 2 parallel; c. 2 series 3 parallel; and d. 6 parallel configuration when it reaches a certain point of  $\Delta T$ . The short circuit current,  $I_{SC}$  and open-circuit voltage,  $V_{OC}$  at points A and B were measured, and maximum power,  $P_{MAX}$  was calculated and presented in Fig. 8(a)~(c) respectively.

It can be seen in Fig. 8(a) that in a 6 series-connected system (blue line), the voltage is multiplied and increase significantly when  $\Delta T$  increase, while compared to 6 parallel-connected system (yellow line), the voltage increases gradually at lowest voltage equaling each module's voltage. Fig. 8(b) shows that

in a series-connected system, the current output was opposite of the voltage output, where the currents in each module are the same and increases gradually when  $\Delta T$  increase, while in a parallel-connected system, the current is multiplied and increase significantly when  $\Delta T$  increase. It can be seen that both systems have a linear relationship between the output voltages and the output currents. In Fig. 8(c), the power of each series and parallel array shows a similar tendency and increasing linearly over  $\Delta T$ .

The findings presented in this experiment support the idea that connecting thermoelectric generators in series would produce better efficiency of the electrical system, as long as the temperature variations remain constant.

#### 4.3. Experiment 3: Sampling on PV-TEG hybrid application

This section presents the experimental on the characteristics of series and parallel connected TEG arrays subject to the non-uniform temperature distribution. An experimental model is provided for each configuration to describe behavior under the open circuit condition and to predict the maximum power output and thermal behavior associated with it. A previous study in Ruzaimi et al. (2018) proof that in a fixed angle of PV panel installation, the temperature distribution tends to be higher towards the direction of the sun from rising to sunset and tends to be higher at its center. A prototype of PV-TEG greenhouse roof system replication was built to assess the real environment parameters on the effect of non-uniform temperature conditions on the TE modules in series and parallel (2-series x 3-parallel) array configuration on the PV backside surface. Data collected on 5 November 2019 between 10:00 AM – 1:00 PM at an open area near the Institute of Advanced Technology, Universiti Putra Malaysia (3°00'70.57"N, 101°72'19.93"E). Fig. 9(a) shows the TE module mounting illustration, Fig. 9(b) shows the measurement method for the experiment purpose, Fig. 9(c) the series-parallel array configuration mounted at area A, B & C; while Fig. 10 was the actual image of the experiment setup.

In this experiment, a 100 W monocrystalline PV panel was used (model PV-YM0902) and using UPM-Solar Noon Locator© software to find the solar panel's optimal direction and elevation to maximize energy generation (Shafie et al., 2018; Khatib et al., 2015). The water-cooling block and surface contact temperature measurement at each TE mounting location (Area A, B & C) were taken by using a temperature data logger (EXTECH Instruments SDL200; sensor K-Type thermocouple). Daily solar irradiance reading (in W/m<sup>2</sup>) was also taken to evaluate the connection between solar irradiance level and temperature during the experiment duration.

The TE hot side temperature was recorded at each area separately to identify the temperature difference at a different area of the PV panel's backside. The thermal distribution images were also taken using Fluke Ti125 thermal imager to observe the temperature distribution and the effect of the TE module contact on the PV panel. The cold side reference was the cooling block water temperature at ambient temperature fluctuating between 34–36°C based on environment condition, which is supposed to be the same in all areas since the water coolant flowing evenly from one block to another. The voltage and current were measured from each module and the entire circuit (between node A to E in Fig. 9(a)).

The temperature and solar irradiance data are presented by the graph shown in Fig. 11(a)–(c) which proves the relativity of solar radiation with PV panel temperature, where the temperature fluctuation is proportional to the solar radiation level. It can be seen that there was a slight difference in the temperature at all the areas being Area A the highest, Area B less high, and Area C the coldest. At 1:00 PM, the  $\Delta T$  dropped as the radiation level decrease due to rainy weather.

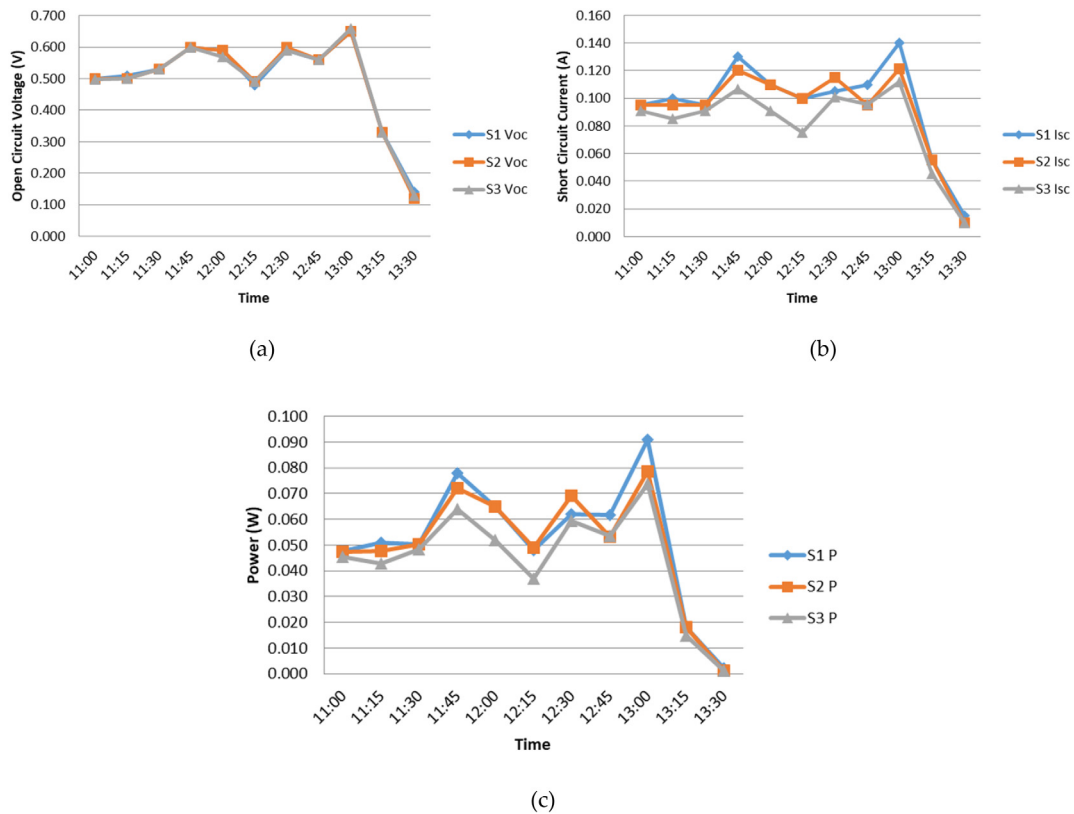


Fig. 12. (a) Open circuit voltage (Voc) for series 1,2 &3 vs. time; (b) Short circuit current (Isc) for series 1,2 &3 vs. time; (c) Output power (P) for series 1,2 &3 vs. time.

The Voc, Isc and P results obtained from the series array of TEGs are shown in Fig. 12(a)–(c) respectively for all the areas. It can be noted that there is a slight difference in the power extracted at each area during the same time, whereby the highest power produced higher at the center of the PV backside surface (Area A) while the less is at Area C (near the PV panel edge). This implies that each area provided a different power capacity under the non-even temperature condition. It should be noted that the wiring and connectors used to connect the TEGs series lead to additional electrical resistance, which in turn reduces the total output power of the TEG array.

The three TEG series string then were connected in parallel into an array which was measured under the same time and radiation. Fig. 13(a) shows the Voc and Isc graph and Fig. 13(b) represent the combined power measured which shows that the produced maximum power is less 33% average less than calculated power, which was what would be available if each series (S1–S3) at area A–C were to be controlled individually. This is also lower than the case of the electrically-in-series. Although some of this power loss is caused by the additional wire and connectors used, the performance comparison between series and parallel case remains valid because of the same number of connections used. It is not as easy to predict the open-circuit voltage of a set of parallel-connected TEGs compared to when connecting the TEGs in series because the value depends on the voltages and internal resistance of the individual TEGs.

Fig. 14 represents the relationship graph between  $\Delta T$  and power. In Area A,  $\Delta T$  is high but the power has not been fully maximized. It is considered that Area A's power was affected by the low current in Area B & C.

Fig. 15 shows the time transition of power and  $\Delta T$ . The solid line is power and the dotted line is  $\Delta T$ . Although  $\Delta T$  of Area A is large, the power is almost the same as the other Area. Hence,

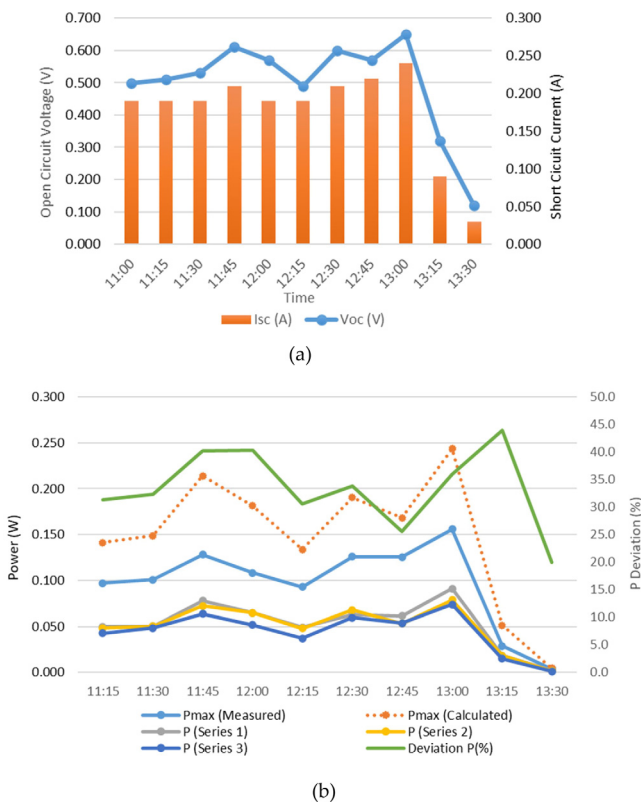


Fig. 13. (a) I–V generated for all series (Area A, B, C) connected in parallel; (b) Power for TE series at area A, B, C, maximum power generated for all series in parallel, and maximum power calculated.

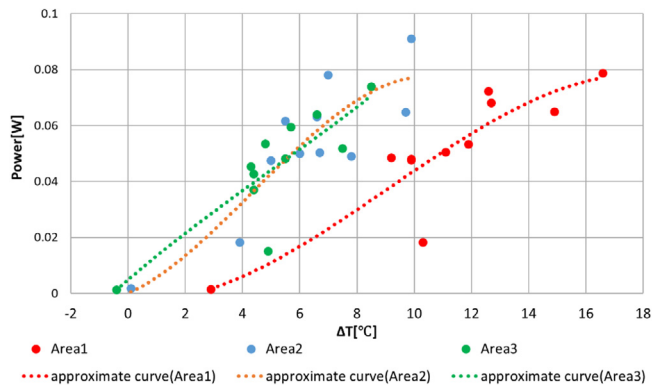


Fig. 14. P vs.  $\Delta T$  for all area connected in parallel under non-even temperature distribution.

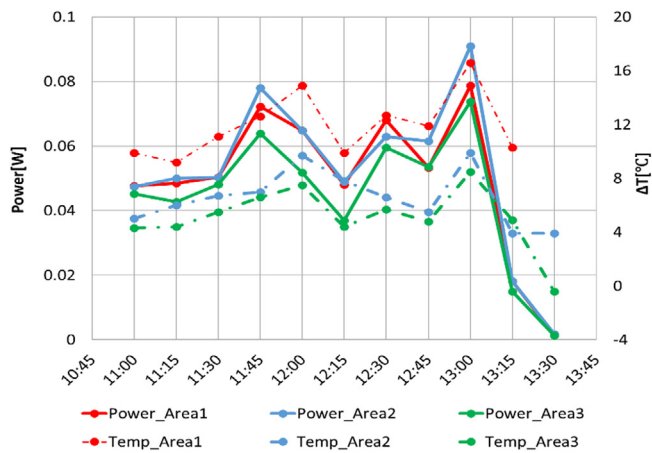


Fig. 15. P vs. time for all area connected in parallel under non-even temperature distribution.

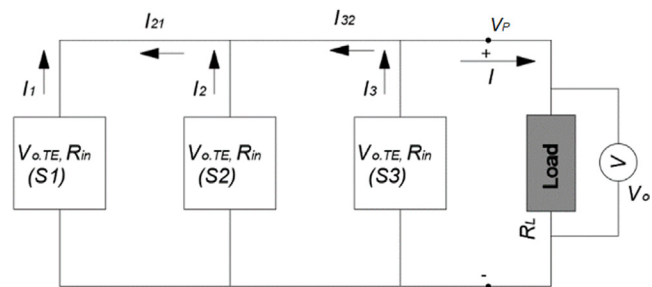


Fig. 16. An equivalent circuit diagram of the experimental setup used to measure the current flowing in parallel connection of a non-uniform thermoelectric circuit.

it is considered that the power of area A was used for power interchange with other areas. The overall effect can be described as negative feedback, for which the TEG series circuit operating at lower and higher  $\Delta T$ , i.e. Series 1 and Series 3 respectively, are drawn towards the middle  $\Delta T$  of Series 2, which is represented in equivalent circuit in Fig. 16. To overcome this feedback, a bypass diode can be implemented, where the diode will be connected in parallel on each TEG series string to avoid the higher current flow to lower current circuits.

The thermal distribution can be seen distributed in non-uniform conditions (Fig. 17), where the temperature is the highest at the center region and decreasing to the edges. However, from the thermal point of view, the temperature distribution contour

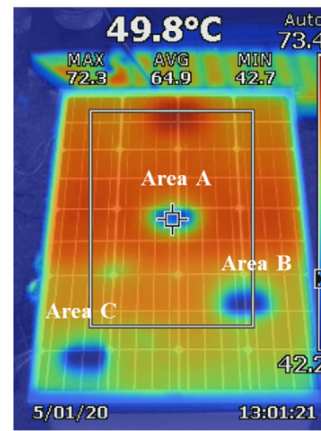


Fig. 17. PV top surface thermal contour shows the TE series circuit cold spot will decrease PV temperature, hence increase the PV module power efficiency.

showed that the TE thermal equalizing influence (Area A, B & C) would bring down the PV panel temperature if all its backside surface mounted with TE modules, at the same time increasing the PV electrical efficiency. In this study, this condition has not been explored and will be investigated in the future to better understand the advantages and disadvantages.

In summary, this study explains the electro-thermal effects that occur in series and parallel arrays of TEG that are exposed to non-uniform temperature gradients. Developed PV-TEG panel prototype models should be modified to include additional physical effects due to temperature imbalance, otherwise, there is a chance of overestimating total power output.

### 5. Conclusions

It is important to choose the highest power output type of TE modules for low-temperature applications such as the PV-TEG hybrid system. TE modules from Custom Thermoelectric module TEC1-12708 have been considered for this application purpose. The non-uniform  $\Delta T$  situation created in the experiment showed a power production drop of an average of 33% from the maximum power that would be available if each TE circuit were controlled individually at the specific area. Experimental data were presented to show that such a problem can impact the performance of a thermoelectric system. The experimental results show that the power lost due to varying conditions (temperature and surface mounting pressure) can be significant and lower in the series-connected array. If there is a temperature difference on the PV surface and TEGs are wired in parallel, TEG power interchange may occur. Hence, it is suggested that bypass diode can overcome this problem. The development of maximum power point tracking (MPPT) controller for the TEG system can be considered to maximize the power output from the circuit. This work analyzed arrays of three TEGs series circuits, however, the results can easily be adapted for a higher number of TEGs. Furthermore, the surface temperature of PV decreases due to heat conduction from the cooling part of TEG can be an advantage to the PV power generation.

### CRedit authorship contribution statement

**Ruzaimi A.:** Investigation, Validation, Writing - original draft. **Shafie. S:** Conceptualization, Methodology, Writing - review & editing, Resources, Supervision. **W.Z.W. Hassan:** Writing - review & editing, Resources. **N. Azis:** Methodology. **M. Effendy Ya'acob:** Methodology. **E. Elianddy:** Methodology. **Aimrun W.:** Methodology, Funding acquisition.

## Declaration of competing interest

The authors declare that they have no known competing financial interests or personal relationships that could have appeared to influence the work reported in this paper.

## Funding

This work is fully funded by the Universiti Putra Malaysia grant number UPM/800-4/11/MRUN/2018/5539220.

## References

- Ariffin, M.R., Shafie, S., Hassan, W.Z.W., Azis, N., Ya'acob, M.E., 2017. Conceptual design of hybrid photovoltaic-thermoelectric generator (PV/TEG) for Automated Greenhouse system. In: 2017 IEEE 15th Student Conference on Research and Development, SCOReD, pp. 309–314. <http://dx.doi.org/10.1109/SCORED.2017.8305373>.
- Ben-Ayoun, Dana, Sadia, Yatir, Gelbstein, Yaniv, 2017. High temperature thermoelectric properties evolution of  $Pb_{1-x}Sn_xTe$  based alloys. *J. Alloys Compd.* 722, 33–38. <http://dx.doi.org/10.1016/j.jallcom.2017.06.075>.
- Çimen, H., Ağaçaçak, A.C., Neşeli, S., Yalçın, G., 2017. Comparison of two different peltiers running as thermoelectric generator at different temperatures. In: 2017 International Renewable and Sustainable Energy Conference, IRSEC, pp. 1–6. <http://dx.doi.org/10.1109/IRSEC.2017.8477309>.
- Gelbstein, Y., Davidow, J., Leshem, E., Pinshow, O., Moisa, S., 2014. Significant lattice thermal conductivity reduction following phase separation of the highly efficient  $Ge_xPb_{1-x}Te$  thermoelectric alloys. *Phys. Status Solidi b* 251, 1431–1437. <http://dx.doi.org/10.1002/pssb.201451088>.
- Hsueh, T.J., Shieh, J.M., Yeh, Y.M., 2015. Hybrid Cd-free CIGS solar cell/TEG device with ZnO nanowires. *Prog. Photovolt., Res. Appl.* 507–512. <http://dx.doi.org/10.1002/pip.2457>.
- Khatib, T., Mohamed, A., Mahmoud, M., Sopian, K., 2015. Optimization of the tilt angle of solar panels for Malaysia. *Energy Sources A* 37, 606–613. <http://dx.doi.org/10.1080/15567036.2011.588680>.
- Lin, J., Liao, T., Lin, B., 2015. Performance analysis and load matching of a photovoltaic thermoelectric hybrid system. *Energy Convers. Manage.* 105, 891–899. <http://dx.doi.org/10.1016/j.enconman.2015.08.054>.
- Madar, Naor, Givon, Tom, Mogilyansky, Dmitry, Gelbstein, Yaniv, 2016. High thermoelectric potential of  $Bi_2Te_3$  alloyed GeTe-rich phases. *J. Appl. Phys.* 120, 035102. <http://dx.doi.org/10.1063/1.4958973>.
- Meroz, Omer, Ben-Ayoun, Dana, Beeri, Ofer, Gelbstein, Yaniv, 2016. Development of  $Bi_2Te_{2.4}Se_{0.6}$  alloy for thermoelectric power generation applications. *J. Alloys Compd.* 679, 196–201. <http://dx.doi.org/10.1016/j.jallcom.2016.04.072>.
- Montecucco, A., Buckle, J., Siviter, J., 2013. A new test rig for accurate nonparametric measurement and characterization of thermoelectric generators. *J. Electron. Mater.* 42, 1966–1973. <http://dx.doi.org/10.1007/s11664-013-2484-4>.
- Montecucco, A., Siviter, J., Knox, A.R., 2012. Simple, fast and accurate maximum power point tracking converter for thermoelectric generators. In: 2012 IEEE Energy Conversion Congress and Exposition, ECCE, pp. 2777–2783. <http://dx.doi.org/10.1109/ECCE.2012.6342530>.
- Montecucco, Andrea, Siviter, Jonathan, Knox, Andrew R., 2014. The effect of temperature mismatch on thermoelectric generators electrically connected in series and parallel. *Appl. Energy* 123, 47–54. <http://dx.doi.org/10.1016/j.apenergy.2014.02.030>.
- Ruzaimi, A., Shafie, S., Hassan, W.Z.W., Azis, N., Ya'acob, M.E., Supeni, E.E., 2018. Photovoltaic panel temperature and heat distribution analysis for thermoelectric generator application. In: 2018 IEEE 5th International Conference on Smart Instrumentation, Measurement and Application, ICSIMA, pp. 1–5. <http://dx.doi.org/10.1109/ICSIMA.2018.8688801>.
- S., Memon, Tahir, K.N., 2018. Experimental and analytical simulation analyses on the electrical performance of thermoelectric generator modules for direct and concentrated quartz-halogen heat harvesting. *Energies* 11, 3315. <http://dx.doi.org/10.3390/en1123315>.
- Sadia, Y., Madar, Naor, Kaler, Ilan, Gelbstein, Y., 2014. Thermoelectric properties of the quasi-binary  $MnSi_{1.73}-FeSi_2$  system. *J. Electron. Mater.* 44, 1637–1643. <http://dx.doi.org/10.1007/s11664-014-3500-z>.
- van Sark, W.G.J.H.M., 2011. Feasibility of photovoltaic – Thermoelectric hybrid modules. *Appl. Energy* 88 (8), 2785–2790. <http://dx.doi.org/10.1016/j.apenergy.2011.02.008>.
- Shafie, S., Azis, N., Ab. Kadir, M.Z.A., Radzi, M.A.M., Zuha, W.H.W., Mustafa, M.A., 2018. High efficiency portable solar generator utilizing optimum solar panel orientation. In: IEEE 5th International Conference on Smart Instrumentation, Measurement and Application 2018, ICSIMA. <http://dx.doi.org/10.1109/ICSIMA.2018.8688811>.
- Tang, Z.B., Deng, Y.D., Su, C.Q., Shuai, W.W., Xie, C.J., 2015. A research on thermoelectric generator's electrical performance under temperature mismatch conditions for automotive waste heat recovery system. *Case Stud. Therm. Eng.* 5, 143–150. <http://dx.doi.org/10.1016/j.csite.2015.03.006>.
- Wang, N., Han, L., He, H., Park, N.H., Koumoto, K., 2011. A novel high performance photovoltaic-thermoelectric hybrid device. *Energy Environ. Sci.* (9), 3676–3679. <http://dx.doi.org/10.1039/C1EE01646F>.
- Zhu, Wei, Deng, Yuan, Wang, Yao, Raza Gulfam, Shengfei Shen, 2016. High-performance photovoltaic-thermoelectric hybrid power generation system with optimized thermal management. *Energy* 100, 91–101. <http://dx.doi.org/10.1016/j.energy.2016.01.055>.